HHS Public Access

Author manuscript

Nat Struct Mol Biol. Author manuscript; available in PMC 2012 August 06.

Published in final edited form as:

Nat Struct Mol Biol. 2011 May ; 18(5): 614–621. doi:10.1038/nsmb.2026.

Cryo–EM structure of the ribosome–SecYE complex in the membrane environment

Jens Frauenfeld[1,2], **James Gumbart**[3], **Eli O. van der Sluis**[1,2], **Soledad Funes**[4], **Marco Gartmann**[1,2], **Birgitta Beatrix**[1,2], **Thorsten Mielke**[5], **Otto Berninghausen**[1,2], **Thomas Becker**[1,2], **Klaus Schulten**[3], and **Roland Beckmann**[1,2,#]

[1] Gene Center, Department for Biochemistry, University of Munich, Feodor–Lynen–Str. 25, 81377 Munich, Germany

[2] Munich Center For Integrated Protein Science (CIPSM), Department of Chemistry and Biochemistry, Butenandtstr. 5–13, 81377 Munich, Germany

[3] Department of Physics, Beckman Institute, University of Illinois at Urbana–Champaign, Urbana, IL, 61801, USA

[4] Departamento de Genética Molecular, Instituto de Fisiología Celular, Circuito Exterior S/N, Ciudad Universitaria, Universidad Nacional Autónoma de México, Mexico, D.F., 04510, Mexico

[5] Ultrastrukturnetzwerk, Max Planck Institute for Molecular Genetics, Ihnestr. 63–73, 14195 Berlin, Institut für Medizinische Physik und Biophysik, Charite–Universitätsmedizin Berlin, Ziegelstrasse 5–9, 10117–Berlin, Germany

Abstract

The ubiquitous SecY/Sec61–complex translocates nascent secretory proteins across cellular membranes and integrates membrane proteins into lipid bilayers. Several structures of mostly detergent solubilized Sec–complexes have been reported. Here, we present a single–particle cryo–electron microscopy structure of the SecYEG complex in a membrane environment at sub–nanometer resolution, bound to a translating ribosome. Using the SecYEG complex reconstituted in a so–called Nanodisc, we could trace the nascent polypeptide chain from the peptidyl transferase center into the membrane. The reconstruction allowed for the identification of ribosome–lipid interactions. The rRNA helix 59 (H59) directly contacts the lipid surface and appears to modulate the membrane in immediate vicinity to the proposed lateral gate of the PCC.

[#]*Corresponding author* Roland Beckmann: beckmann@lmb.uni-muenchen.de Tel: +49 89 2180 76900 Fax: +49 89 2180 76945.

Author contributions

J.F. prepared the sample, collected the EM data, performed the 3D reconstruction and built the molecular model, J.C.G. did the MDFF and the MD simulations. E.O.v.d.S., S.F. and B.B. contributed to the purification of SecYEG, M.G. contributed to the data processing. T.M. and O.B. contributed to the EM data collection. T.B. contributed to model building and interpretation. All authors contributed to the study design and to writing the manuscript.

Supplementary Information

Note: Supplementary information is available on the Nature Structural & Molecular Biology website.

Accession codes

Coordinates of the atomic model and the cryo–EM map have been deposited in the PDB (to be announced XXX) and in the 3D–EM database (EMD–1858), respectively.

Based on our map and molecular dynamics simulations we present a model of a signal anchor–gated PCC in the membrane.

Introduction

The vast majority of proteins designated to be secreted or to be integrated into the membrane bilayer has to pass the ubiquitous protein–conducting channel (PCC), termed Sec61 complex in eukaryotes or SecYEG in prokaryotes[1]. In the cotranslational mode, when the hydrophobic signal sequence or signal anchor (SA) of a nascent polypeptide chain emerges from the ribosome, the ribosome–nascent chain complex (RNC) is targeted to the membrane by the signal recognition particle (SRP) and the SRP–receptor (SR)[2]. After transfer from the SRP system to the PCC, the ribosome continues translation while the nascent polypeptide is directly guided from the ribosomal exit tunnel into the ribosome–bound SecY/61 complex for membrane translocation or integration.

The PCC is conserved amongst all organisms and several crystal structures of detergent–solubilized PCCs have been reported[3–6], sharing a common core of twelve transmembrane (TM) helices. This core consists of one large and two small subunits, termed SecY/Sec61α, SecE/Sec61γ and the less conserved SecG/Sec61β, respectively. In *Escherichia Coli (E. coli)*, SecY is composed of two pseudo–symmetric halves comprising the N–terminal TM1–TM5 and C–terminal TM6–TM10. SecY is flanked by the clamp–like protein SecE, composed of three TM helices and an amphipathic helix, and SecG consisting of two TM–helices. The PCC may open both, perpendicular to the plane of the membrane for the translocation of soluble polypeptides across the membrane, and laterally for the integration of TM helices into the membrane. To that end, the two clam shell–like halves of SecY have been suggested to open on one side in order to form a lateral gate for accommodation of the signal sequence or the SA[4–7]. Consistent with this idea, three recent crystal structures of SecYE show a partial opening of the lateral gate[4–6]. After the gating event, the polypeptide is thought to use the central hourglass–shaped aqueous vestibule of the Sec complex as a conduit for translocation[8]. The central plug helix 2a of SecY would move and the central hydrophobic pore ring would provide a flexible seal to avoid ion leakage across the membrane[1]. Although a low resolution cryo–EM structure of a programmed ribosome–SecYEG complex was interpreted to comprise two copies of the SecYEG complex forming a joint pore[9], more recent biochemical, structural, and simulation data showed that a single copy of the Sec complex is most likely forming the active PCC[10–13,14]. All 3D–structures of the PCC bound to the ribosome, however, were obtained using detergent solubilized Sec–complexes[6,9–11,13,15–19]. It has been shown that, in principle, the PCC can be active in detergent solution[20], however, it is not clear to what extent the absence of the lipid bilayer may influence the structure and the activity of the PCC. Thus, the conformation of the ribosome–Sec–complex in its natural environment remains to be elucidated. Furthermore, questions regarding PCC–mediated membrane protein integration or assembly can only be addressed in the presence of a bilayer.

Therefore, a routine approach for the visualization of membrane proteins within a membrane environment is highly desirable. Traditional 2D–electron crystallography[21] and the more

recent single–particle cryo–EM approach called RSC[22] are limited by the difficulty to generate 2D crystals and the rather low resolution, respectively. Here, we report on a new approach to obtain subnanometer–resolution structures of membrane protein complexes in a lipid bilayer environment. We integrated the *E. coli* SecYEG complex into high density lipoprotein (HDL) particles, also termed Nanodiscs, a defined and soluble nano–scale phospholipid bilayer stabilized by a mutant form of apolipoprotein A1[23,24] and subjected it after reconstitution with RNCs to high–resolution single–particle cryo–EM.

Results and Discussion

Reconstruction of the ribosome–Nd–SecYEG complex

We purified *E. coli* RNCs[25] carrying an elongation arrested nascent chain of 118 amino acid residues. The first 102 residues represented the N–terminus of the membrane protein FtsQ, preceded by an HA– and a His–tag for affinity purification. This type II membrane protein contains an N–terminal signal–anchor transmembrane (TM) helix that was shown to insert co–translationally into the membrane and to remain in contact with SecY and lipids after insertion[26]. Nanodiscs were reconstituted with a mutant form of apolipoprotein A1 (Apo–A1 Δ1–43) as described before[23] using *E. coli* total lipid extract in the absence or presence of purified recombinant *E. coli* SecYEG complex. This resulted in Nanodiscs containing only lipids (Nd–E) or SecYEG–containing Nanodiscs (Nd–SecYEG).

Nascent FtsQ–carrying RNCs were then reconstituted with an excess of Nd–SecYEG, and used in binding assays to test whether the RNC–Nanodisc interaction was dependent on SecYEG. Stable binding of RNCs was observed only in the presence of Nd–SecYEG (Fig. 1a), indicating that neither the ribosome nor the SA domain of the nascent FtsQ could interact with, or insert into the lipid bilayer in a SecYEG–independent manner. We, therefore, concluded that the reconstituted complexes indeed represented RNC–Nd–SecYEG complexes.

The cryo–EM reconstruction of this complex shows the appearance of a programmed 70S ribosome at 7.1 Å resolution with an additional disc–like density beneath the ribosomal exit site (Fig. 1b, Supplementary Fig. 1). This density had a diameter of 10–12 nm and a height of about 4–5 nm, tethered by several contacts to the ribosome. The appearance of a clear tRNA density in the P–site confirmed the presence of the nascent FtsQ chain as peptidyl–tRNA. It was possible to visualize the density of the nascent chain within the ribosomal exit tunnel reaching from the peptidyl–transferase center (PTC) into the Nd–SecYEG density (Fig. 1c). The ribosome contacted the Nd–SecYEG density via several connections, yet, leaving a gap on one side of about 15–25 Å between the ribosome and the Nd–SecYEG. This gap is in agreement with data obtained from detergent solubilized complexes[15,16,19], indicating the lack of a seal between the ribosome and the membrane–embedded PCC[27]. The gap suffices to provide the space required for folding or egress of cytosolic domains of membrane proteins.

To interpret the cryo–EM map on a molecular level, we docked crystal structures and molecular models into the density and applied molecular dynamics flexible fitting (MDFF)[28], resulting in a complete molecular model for the 70S–RNC–Nd–SecYEG

complex (Fig. 1d, Supplementary Material Methods). This model was used as a starting point for a 16 ns molecular dynamics (MD) simulation.

Structure of the Nanodisc

The region of the map representing the Nanodisc was expected to consist of a lipid bilayer with an upper and lower membrane leaflet stabilized by two belt–like Apo–A1 Δ1–43 molecules surrounding it. The observed density indeed shows the characteristic dimension of a lipid bilayer with a thickness of about 43 Å (Fig. 2a). Strong electron density for the phospholipid headgroups was present that could be distinguished from the very weak density for the region occupied by the acyl chains of the fatty acids (Fig. 2a). This distribution resembles that observed in membrane–containing viruses[29,30] and in liposomes[31]. In contrast to the phosphate headgroups, the acyl chains of the lipids yield very weak electron density due to their composition of low– contrast carbon and hydrogen atoms. The overall dimensions of the electron density representing the Nanodisc are in good agreement with a molecular model for nascent discoidal HDL, determined using hydrogen–deuterium exchange mass spectrometry or x–ray crystallography of the protein alone[24,32,33]. The outer ring of the Nanodisc, suggested to be composed of two parallel copies of Apo–A1 Δ1–43, also displays a stronger density than the lipid acyl chains (Fig. 2). However, the density did not allow for the resolution of the protein belts. Nevertheless, we used a current molecular model for Apo–A1[32] and also lipids to complete our modelling effort for the MD simulation. Fragmented density outside the main disc may be a result of heterogeneity of the disc diameter or of the presence of non–lipidated N–terminal regions of Apo– A1 Δ1–43, respectively. Within the bilayer, we found rod–like structures directly beneath the ribosomal tunnel exit, apparently representing the TM helices of the SecYEG complex (Fig. 2, Supplementary Fig. 1c). The resolution of the Nanodisc appears to be somewhat lower as that of the ribosome. However, the appearance of the rod–like densities representing alpha–helical regions of SecYE indicates that the resolution for the SecYE complex in the Nanodisc is in the sub–nanometer range. Our observation shows that the overall dimensions of the membrane–protein–containing Nanodisc resemble those of a small circular lipid bilayer which can be subjected to structure analysis at sub–nanometer resolution.

Model of the ribosome–SecYE complex and contacts

Based on the previously observed contacts of the cytosolic loops L8/9 and L6/7 of SecY/Sec61 to the ribosome[10,11,13] (Supplementary Fig. 2), we fitted a homology model of *E. coli* SecYE into our density by MDFF (Fig. 3a). Using the structure of SecYE in the SecYE–SecA complex[4] as a template, the C–terminal half of SecY fitted remarkably well and only small adjustments of the N–terminal TM helices of SecY were necessary (Fig. 3a, b; Supplementary Fig. 3a, b). The position of the short plug helix 2a remained essentially identical to that observed in the SecYE–SecA structure. The N–terminal TM helices of SecE were placed into two additional rod– like densities, guided by the 2D crystal structure of the SecYEG complex[34,35] (Supplementary Fig. 3c, d). Although we observed some density also in the region where SecG was expected[4] (Fig. 2b, Supplementary Figs 3d, e, 12), we could not unambiguously identify its exact position, indicating a higher degree of flexibility. Notably, the fitted model left a rod–like density in the proposed lateral gate of SecY unaccounted for, that we interpreted as the inserted SA helix of FtsQ (Fig. 2, Supplementary

Fig. 3d). The MD simulation revealed a stable behaviour of the fitted model of the PCC (Supplementary Fig. 4a) that, together with a cross–correlation analysis of the quality of the fit, supports its accuracy (Supplementary Table 1). Furthermore, the connections between SecYE and the ribosome were maintained throughout the simulation (Supplementary Fig. 5), and the position of the SA TM domain was stable with respect to the PCC (Supplementary Fig. 4b).

A multitude of contacts were identified between the ribosome and SecYE as well as lipids (Fig. 3, Supplementary Tables 2–6). The cytoplasmic loops L8/9 and L6/7 of SecY reached into the ribosomal exit tunnel and contacted ribosomal RNA (rRNA) helices H50/53/59 and H6/24/50, respectively (Fig. 3a, c, e, f). Furthermore, both loops also contacted the ribosomal protein L23 in different regions (Supplementary Tables 2–6). Notably, the binding mode we observe in the presence of a signal sequence and a lipid bilayer is very similar to the mode found in inactive complexes and in detergent solution[10,11,13,14]. Thus, this interaction appears to represent the canonical binding mode of the Sec–complex to the universal ribosomal adaptor site for both prokaryotic and eukaryotic complexes. An additional contact was likely to represent the C–terminus of SecY, contacting ribosomal protein L24 and rRNA helices H24/50 (Fig. 3a, e, f). A contribution of the SecY C–terminus to ribosome binding is in agreement with recent findings for both the bacterial[14] and the eukaryotic system[13], as well as mutational studies revealing translocation defects of C–terminally truncated SecY[36]. In addition to SecY, SecE contributes to the interaction of the PCC with the ribosome (Fig. 3c, e, f), consistent with previous data[10,11,13,14]. We observed several contacts between the N–terminus as well as the amphipathic helix of SecE and the ribosomal adaptor site proteins L23 and L29, respectively. A stretch of conserved residues in the amphipathic helix of SecE[37] appeared to be involved in contacting both SecY and L23/L29. While in agreement with several previous studies[10–13,14], these findings are difficult to reconcile with the interpretation by Mitra et al.[9]

Interestingly, the Nd–SecYEG–bound ribosome did not only interact with the PCC but also with lipids. A strong density between rRNA helix H59 and the disc is apparently mediated by a direct contact to lipid headgroups (Fig. 1b–d, Fig. 3d, Supplementary Movie M1), which is in agreement with previous observations[11,14]. In addition, L24 showed a strong contact with the Nd–SecYEG density that may also involve lipids. After the initial fitting of molecular models, a molecular dynamics simulation of the ribosome–Nd–SecYE–lipid model was performed, containing a lipid bilayer of 75% phosphatidylethanolamine and 25% phosphatidylglycerol, mimicking the composition of the bacterial plasma membrane.

Initially, we fitted a flat lipid bilayer into the Nanodisc density; however, shortly after the start, the simulation showed a stable attraction between lipids and rRNA helix H59 (Supplementary Movie M1). The resulting lipid distribution resembled the electron density remarkably well, indicating that H59 is indeed capable of establishing another interaction site between ribosome and membrane–PCC–complex (Fig. 3d). In contrast, the additional interactions between L24 and lipids, which were also in good agreement with our electron density, were intermittent, as L24 was seen to preferentially interact with SecY/nascent chain later in the simulation. The direct interaction of the ribosome with the lipid bilayer, in addition to the SecYE contacts, may explain the rigid positioning of the entire disc with

respect to the ribosome and the asymmetrical position of the SecY complex in the disc. Taken together, a multitude of contacts between ribosome and the C–terminal half of the PCC as well as lipids results in a robust coordination of the ribosome with respect to the membrane surface (Fig. 3e, f). The observed conformation orients the ribosomal surface around the tunnel exit almost parallel to the surface of the membrane while leaving a distance of about 20 Å on one side (Supplementary Fig. 6). The position of the lateral gate of SecYEG with respect to the ribosomal–PCC contacts would easily facilitate egress of cytoplasmic domains of nascent peptides alongside the H59 contact away from the main interaction sites.

Model and path of the translocating polypeptide chain

The resolution of the electron density allowed for the tracing of the nascent polypeptide chain from the PTC through the ribosomal exit tunnel (Fig. 1c). Furthermore, in the membrane, one rod–like density at the lateral gate of the PCC is best explained by the presence of the inserted SA of FtsQ (Fig. 4d, e, Supplementary Fig. 3b). After passing the central constriction of the ribosomal tunnel with an unaltered loop region of L22 (Supplementary Fig. 7a), the nascent chain engages in a number of contacts in the lower half of the tunnel involving the ribosomal proteins L23, L24 and SecY (Fig. 4a, Supplementary Tables 2–6). Noteworthy, protein loops participate in all of these contacts and undergo conformational changes when compared to structures of inactive complexes. The conserved loop of L23 that reaches up the tunnel wall has been suggested to constitute a potential interaction site for nascent proteins[38], possibly leading to an inside–outside signalling of the nascent chain[39]. In our complex, the tip of L23 (Fig. 4b) indeed shifts down when compared to empty ribosomes analyzed by cryo–EM or x–ray crystallography (Supplementary Fig. 7b). In the immediate vicinity, the nascent chain subsequently contacts the tip of L6/7 of SecY that embraces the nascent chain. This may indicate a putative role of L6/7 as a sensor for the presence and/or the nature of the nascent chain inside the ribosomal tunnel. Interestingly, when interacting with an empty ribosome, a different conformation of L6/7 of SecY was observed to occlude the tunnel[10] (Supplementary Fig. 8). This might be of functional relevance after termination and re–initiation of translation when a newly arriving nascent chain could regulate dissociation of the PCC from the ribosome by interfering with the L6/7. When finally exiting the ribosomal tunnel, the nascent chain contacts the exposed beta–hairpin of L24 (Fig. 4c). This hairpin loop is also bent downwards to probably contact the lipid surface and the C–terminus of SecY. Taken together, the nascent chain is carefully guided by protein loops through the ribosomal tunnel to its site of insertion into the PCC.

At the present resolution we could not trace the path of the complete NC within the PCC. Yet, we aimed at building a full model and therefore generated a hypothetical path of the NC within the SecY core, based on biochemical data published before[8] and in agreement with our SecY model. Therefore, after fitting the TM helices of SecY, we simply extended the NC model from the cytoplasmic to the periplasmic side through the central pore[8], as indicated by a dashed line (Fig. 4a). In our SecYE model, the central opening leaves enough space for an extended polypeptide chain to pass while, at the same time, a substantial flow of ions would be prevented in the presence of a translocating peptide.

To obtain a complete model for MD simulations we then connected the NC model (dashed line) with the SA within the proposed lateral gate of the PCC, resulting in the loop–like arrangement expected for a type II membrane protein. Adjusting the SecYE complex from the SecA–activated, pre–open conformation[4] of the template to our map resulted in a laterally open conformation (Supplementary Fig. 9). Interestingly, mainly the gate helices and the N–terminal half of SecY undergo movements, while the TMs of the C–terminal half superimpose well with the structure of the pre–open state (Supplementary Fig. 9a). This conformation permitted the fitting of the additional SA helix into the rod–like density within the lateral gate (Fig. 4, Supplementary Fig. 1c, 3b, 9, 10).

The resulting model provides a plausible scenario with an overall arrangement that is in agreement with previous biochemical and structural data. In this model the SA is exposed towards the lipid bilayer, yet it remains tightly enframed by TM2b, TM7 and TM8 of SecY that may indeed act as the lateral gate for TM domains for insertion into the membrane[3,4,40]. This SA position explains chemical cross–link data that indicate, at a similar chain length, close proximity of the SA of FtsQ to both SecY and lipids[26]. Upon further chain elongation, complete release of the SA from SecY is likely to be triggered by additional factors such as YidC[41,42]. The position of the SA in the lateral gate is also consistent with contacts to conserved hydrophobic residues of SecY TMs 2, 7 and 8[5,8] (Fig. 4 d, e) as well as with contacts to residues that can be cross–linked to the signal sequence of proOmpA[8]. During the MD simulation, the SA remained stable with respect to SecYE (Supplementary Fig. 4). Notably, virtually no hydrogen bonds, but mainly hydrophobic interactions were observed between the SA and SecY (Supplementary Fig. 10 and tables). Whereas a substantial number of hydrogen bonds would reduce the TM domain's ability to exit into the bilayer, hydrophobic interactions would be in agreement with partitioning according to the TM domain's hydrophobicity. Although we cannot exclude limited flexibility of the SA, the robust density argues in favour of high occupancy in the observed position. Taken together, this indicates that the SA is in a reasonable and meaningful position in the structure. The positively charged N–terminus of the FtsQ SA could remain on the cytosolic side, stabilized by additional interactions with either the phospholipid headgroups or the negatively charged phosphate backbone of the nearby rRNA helix H59. At the same time, the position of the SA would prevent phospholipids from entering the center of the PCC. In conclusion, the suggested TM helix at the interface between the lateral gate of SecY and the lipid bilayer as positioned in our model may represent an intermediate step of TM integration into the membrane.

Insertion of a TM domain into the membrane

Both our map and the MD simulation revealed a stable attraction between lipids and rRNA helix H59 (Fig. 3d, Fig. 5a, Supplementary Fig. 11, Supplementary Table 7). Notably, this lipid–H59 interaction resulted in a redistribution of the lipids which affects the immediate vicinity of the suggested TM domain insertion region (Fig. 5a–c). The lateral diffusion of lipids is decreased around H59 and the cytoplasmic leaflet of the membrane is less ordered. Similar findings have been reported in a number of recent studies, highlighting that RNA–lipid interactions are based on electrostatic attractions[43–46]. Interestingly, RNA binding to lipid bilayers may influence and change the bilayer state[45]. Most notably, RNAs can even

insert into bilayers and perturb membrane permeability[44]. In addition, it has been shown that RNA–lipid binding may lead to lateral segregation and formation of domains with different compositions in the lipid bilayer[43]. This is in good agreement with our cryo–EM–density/MD–simulation finding that ribosomal rRNA H59 indeed attracts the charged headgroups (Supplementary Table 7), leading to a disorder in the lipid bilayer in proximity to the lateral gate of SecY. We speculate that this induced disorder may favour membrane insertion of TM domains by decreasing the energy barrier for the TM to access the hydrophobic core of the lipid bilayer through the layer of charged head groups. This is supported by the idea that insertion efficiency is determined by the energetic cost of distorting the bilayer in the vicinity of the TM helix, as predicted by MD simulations[47]. By interacting with positively charged N–terminal residues of TM domains, there might even be a contribution of H59 to the correct orientation of TM domains according to the positive–inside rule[48].

When comparing our model to the bacterial RNC–SRP complex[25], the positions of the SA domain are in close proximity to each other (Fig. 5d, Supplementary Fig. 12). Notably, apart from the previously observed removal of the NG–domain from its L23 binding–site[25], only minor conformational adjustments would be required for a concomitant binding of SRP and the SecYEG complex to the ribosome. For transfer from the targeting system to the PCC, the SA could slide from the SRP54 M–domain directly into the lateral gate/lipid region of the SecYEG complex (Fig. 5e, Supplementary Fig. 12). A virtually continuous hydrophobic environment for the insertion of the TM domain into the lipid phase would be provided. The hydrophilic residues that follow the SA would then be oriented in the hydrophilic central conduit of the channel, resulting in the loop–like insertion of the nascent polypeptide (Fig. 5d–f).

Conclusions

Our sub–nanometer resolution cryo–EM structure of the bacterial ribosome–SecYEG complex in a Nanodisc allows for the molecular interpretation of a membrane protein, the SecYEG complex, in its natural lipid bilayer environment. We suggest an insertion intermediate of a type II membrane protein using the proposed lateral gate of the SecYEG complex for partitioning into the lipid phase. Molecular dynamics simulations based on our structure reveal stable interactions between ribosomal RNA and the membrane that may contribute to the insertase activity of the PCC. Using nascent polytopic membrane proteins, future studies will address the mechanism of more complex membrane insertion events. This method may provide a general approach to visualize functional membrane proteins in the lipid environment by high–resolution single particle cryo–EM.

Methods

RNCs, the *E. coli* SecYEG complex and Nanodiscs (Nd–E, Nd–SecYEG) were prepared essentially as described before[23,25,49]. RNC–Nd–SecYEG complexes were reconstituted by incubating purified RNCs with an excess of Nd–SecYEG for 15 min at 37°C followed by 15 min on ice. Binding assays were done by centrifugation followed by SDS–PAGE analysis of supernatant and pellet fractions. Prior to application to carbon–coated EM grids,

reconstituted RNC–Nd–SecYEG complexes were pelleted and then vitrified. Cryo–EM data collection on plates was done on a 300 kV Polara FEG cryo–microscope, FEI; data were digitized and then processed using the Software Spider[25,50]. Sorting of the dataset according to the presence of the Nanodisc resulted in a final population of 85,664 particles that were used for a 3D reconstruction with a resolution of 7.1 Å according to the FSC 0.5 criterion. For the molecular model, we used available crystal structures either directly (*E. coli* 70S ribosome) or as templates for homology modelling (SecYEG complex), followed by fitting into the density by molecular dynamics flexible fitting (MDFF)[28]. The molecular dynamics (MD) simulations were done using the GPU–accelerated version of NAMD on the Lincoln cluster at NCSA[51]. The analysis of the simulation was done with VMD[52]. Figures were prepared using Chimera[53] and Adobe CS3.

Supplementary Material

Refer to Web version on PubMed Central for supplementary material.

Acknowledgements

We thank B. Seidelt for help with the RNC preparation, J.P. Armache for help with data processing, S. Feuerstein (ISB–3, Structural Biochemistry, Forschungszentrum Jülich, 52425 Jülich, Germany) for providing the plasmid encoding the apolipoprotein construct, J. Buerger and C. Ungewickell for help with the electron microscopy and D. Wilson for critical discussions. This research was supported by a Boehringer Ingelheim Fonds fellowship (to J.F.), by an Alexander von Humboldt Foundation fellowship and a Human Frontiers Science Program long term fellowship (to E.O.v.d.S.), by a Dr. Klaus Römer–Stiftung fellowship (to T.B.), by grants from the Deutsche Forschungsgemeinschaft SFB594 and SFB646 (to R.B.), SFB 740 (to T.M.), by NIH grants P41–RR05969, R01–GM067887 (to K.S.), by NSF grant PHY0822613 (to K.S.) and by a Humboldt award (to K.S.), by the European Union and Senatsverwaltung für Wissenschaft, Forschung und Kultur Berlin (UltraStructureNetwork, Anwenderzentrum). Computer time for MD simulations and MDFF was provided through an NSF Large Resources Allocation Committee grant MCA93S028.

References

1. Rapoport TA. Protein translocation across the eukaryotic endoplasmic reticulum and bacterial plasma membranes. Nature. 2007; 450(7170):663–669. [PubMed: 18046402]
2. Halic M, Beckmann R. The signal recognition particle and its interactions during protein targeting. Curr Opin Struct Biol. 2005; 15(1):116–125. [PubMed: 15718142]
3. Van den Berg B, et al. X–ray structure of a protein–conducting channel. Nature. 2004; 427(6969): 36–44. Epub 2003 Dec 2003. [PubMed: 14661030]
4. Zimmer J, Nam Y, Rapoport TA. Structure of a complex of the ATPase SecA and the protein–translocation channel. Nature. 2008; 455(7215):936–943. [PubMed: 18923516]
5. Tsukazaki T, et al. Conformational transition of Sec machinery inferred from bacterial SecYE structures. Nature. 2008; 455(7215):988–991. [PubMed: 18923527]
6. Egea PF, Stroud RM. Lateral opening of a translocon upon entry of protein suggests the mechanism of insertion into membranes. Proc Natl Acad Sci U S A. 107(40):17182–17187. [PubMed: 20855604]
7. du Plessis DJ, Berrelkamp G, Nouwen N, Driessen AJ. The lateral gate of SecYEG opens during protein translocation. J Biol Chem. 2009; 284(23):15805–15814. [PubMed: 19366685]
8. Osborne AR, Rapoport TA. Protein translocation is mediated by oligomers of the SecY complex with one SecY copy forming the channel. Cell. 2007; 129(1):97–110. [PubMed: 17418789]
9. Mitra K, et al. Structure of the E. coli protein–conducting channel bound to a translating ribosome. Nature. 2005; 438(7066):318–324. [PubMed: 16292303]
10. Menetret J–F, et al. Ribosome Binding of a Single Copy of the SecY Complex: Implications for Protein Translocation. Molecular Cell. 2007; 28(6):1083–1092. [PubMed: 18158904]

11. Menetret JF, et al. Single copies of Sec61 and TRAP associate with a nontranslating mammalian ribosome. Structure. 2008; 16(7):1126–1137. [PubMed: 18611385]
12. Kalies KU, Stokes V, Hartmann E. A single Sec61–complex functions as a protein–conducting channel. Biochim Biophys Acta. 2008; 1783(12):2375–2383. [PubMed: 18778738]
13. Becker T, et al. Structure of Monomeric Yeast and Mammalian Sec61 Complexes Interacting with the Translating Ribosome. Science. 2009
14. Gumbart J, Trabuco LG, Schreiner E, Villa E, Schulten K. Regulation of the protein–conducting channel by a bound ribosome. Structure. 2009; 17(11):1453–1464. [PubMed: 19913480]
15. Beckmann R, et al. Architecture of the protein–conducting channel associated with the translating 80S ribosome. Cell. 2001; 107(3):361–372. [PubMed: 11701126]
16. Beckmann R, et al. Alignment of conduits for the nascent polypeptide chain in the ribosome–Sec61 complex. Science. 1997; 278(5346):2123–2126. [PubMed: 9405348]
17. Menetret JF, et al. Architecture of the ribosome–channel complex derived from native membranes. J Mol Biol. 2005; 348(2):445–457. [PubMed: 15811380]
18. Morgan DG, Menetret JF, Neuhof A, Rapoport TA, Akey CW. Structure of the mammalian ribosome–channel complex at 17A resolution. J Mol Biol. 2002; 324(4):871–886. [PubMed: 12460584]
19. Menetret J, et al. The structure of ribosome–channel complexes engaged in protein translocation. Mol Cell. 2000; 6(5):1219–1232. [PubMed: 11106759]
20. Matlack KE, Plath K, Misselwitz B, Rapoport TA. Protein transport by purified yeast Sec complex and Kar2p without membranes. Science. 1997; 277(5328):938–941. [PubMed: 9252322]
21. Raunser S, Walz T. Electron crystallography as a technique to study the structure on membrane proteins in a lipidic environment. Annu Rev Biophys. 2009; 38:89–105. [PubMed: 19416061]
22. Wang L, Sigworth FJ. Structure of the BK potassium channel in a lipid membrane from electron cryomicroscopy. Nature. 2009; 461(7261):292–295. [PubMed: 19718020]
23. Alami M, Dalal K, Lelj–Garolla B, Sligar SG, Duong F. Nanodiscs unravel the interaction between the SecYEG channel and its cytosolic partner SecA. EMBO J. 2007; 26(8):1995–2004. [PubMed: 17396152]
24. Shih, AY.; Freddolino, PL.; Arkhipov, A.; Sligar, SG.; Schulten, K. Current Topics in Membranes: Computational Modeling of Membrane Bilayers. Elsevier; 2008. Molecular modeling of the structural properties and formation of high–density lipoprotein particles.; p. 313-342.
25. Halic M, et al. Following the signal sequence from ribosomal tunnel exit to signal recognition particle. Nature. 2006; 444(7118):507–511. [PubMed: 17086193]
26. Urbanus ML, et al. Sec–dependent membrane protein insertion: sequential interaction of nascent FtsQ with SecY and YidC. EMBO Rep. 2001; 2(6):524–529. [PubMed: 11415986]
27. Hamman BD, Chen JC, Johnson EE, Johnson AE. The aqueous pore through the translocon has a diameter of 40–60 A during cotranslational protein translocation at the ER membrane. Cell. 1997; 89(4):535–544. [PubMed: 9160745]
28. Trabuco LG, Villa E, Mitra K, Frank J, Schulten K. Flexible fitting of atomic structures into electron microscopy maps using molecular dynamics. Structure. 2008; 16(5):673–683. [PubMed: 18462672]
29. Cockburn JJ, et al. Membrane structure and interactions with protein and DNA in bacteriophage PRD1. Nature. 2004; 432(7013):122–125. [PubMed: 15525993]
30. Laurinmaki PA, Huiskonen JT, Bamford DH, Butcher SJ. Membrane proteins modulate the bilayer curvature in the bacterial virus Bam35. Structure. 2005; 13(12):1819–1828. [PubMed: 16338410]
31. Tilley SJ, Orlova EV, Gilbert RJ, Andrew PW, Saibil HR. Structural basis of pore formation by the bacterial toxin pneumolysin. Cell. 2005; 121(2):247–256. [PubMed: 15851031]
32. Wu Z, et al. The refined structure of nascent HDL reveals a key functional domain for particle maturation and dysfunction. Nat Struct Mol Biol. 2007; 14(9):861–868. [PubMed: 17676061]
33. Borhani DW, Rogers DP, Engler JA, Brouillette CG. Crystal structure of truncated human apolipoprotein A–I suggests a lipid–bound conformation. Proc Natl Acad Sci U S A. 1997; 94(23): 12291–12296. [PubMed: 9356442]

34. Breyton C, Haase W, Rapoport TA, Kuhlbrandt W, Collinson I. Three–dimensional structure of the bacterial protein–translocation complex SecYEG. Nature. 2002; 418(6898):662–665. [PubMed: 12167867]
35. Collinson I. The structure of the bacterial protein translocation complex SecYEG. Biochem Soc Trans. 2005; 33(Pt 6):1225–1230. [PubMed: 16246086]
36. Chiba K, Mori H, Ito K. Roles of the C–terminal end of SecY in protein translocation and viability of Escherichia coli. J Bacteriol. 2002; 184(8):2243–2250. [PubMed: 11914356]
37. Murphy CK, Beckwith J. Residues essential for the function of SecE, a membrane component of the Escherichia coli secretion apparatus, are located in a conserved cytoplasmic region. Proc Natl Acad Sci U S A. 1994; 91(7):2557–2561. [PubMed: 8146153]
38. Houben EN, Zarivach R, Oudega B, Luirink J. Early encounters of a nascent membrane protein: specificity and timing of contacts inside and outside the ribosome. J Cell Biol. 2005; 170(1):27–35. [PubMed: 15983062]
39. Bornemann T, Jockel J, Rodnina MV, Wintermeyer W. Signal sequence–independent membrane targeting of ribosomes containing short nascent peptides within the exit tunnel. Nat Struct Mol Biol. 2008; 15(5):494–499. [PubMed: 18391966]
40. Gumbart J, Schulten K. Structural determinants of lateral gate opening in the protein translocon. Biochemistry. 2007; 46(39):11147–11157. [PubMed: 17760424]
41. Scotti PA, et al. YidC, the Escherichia coli homologue of mitochondrial Oxa1p, is a component of the Sec translocase. Embo J. 2000; 19(4):542–549. [PubMed: 10675323]
42. van der Laan M, Houben EN, Nouwen N, Luirink J, Driessen AJ. Reconstitution of Sec–dependent membrane protein insertion: nascent FtsQ interacts with YidC in a SecYEG–dependent manner. EMBO Rep. 2001; 2(6):519–523. [PubMed: 11415985]
43. Michanek A, Kristen N, Hook F, Nylander T, Sparr E. RNA and DNA interactions with zwitterionic and charged lipid membranes – a DSC and QCM–D study. Biochim Biophys Acta. 1798(4):829–838. [PubMed: 20036213]
44. Khvorova A, Kwak YG, Tamkun M, Majerfeld I, Yarus M. RNAs that bind and change the permeability of phospholipid membranes. Proc Natl Acad Sci U S A. 1999; 96(19):10649–10654. [PubMed: 10485880]
45. Janas T, Yarus M. Specific RNA binding to ordered phospholipid bilayers. Nucleic Acids Res. 2006; 34(7):2128–2136. [PubMed: 16641318]
46. Marty R, N'Soukpoe–Kossi CN, Charbonneau DM, Kreplak L, Tajmir–Riahi HA. Structural characterization of cationic lipid–tRNA complexes. Nucleic Acids Res. 2009; 37(15):5197–5207. [PubMed: 19561199]
47. Jaud S, et al. Insertion of short transmembrane helices by the Sec61 translocon. Proc Natl Acad Sci U S A. 2009; 106(28):11588–11593. [PubMed: 19581593]
48. von Heijne G. The distribution of positively charged residues in bacterial inner membrane proteins correlates with the trans–membrane topology. EMBO J. 1986; 5(11):3021–3027. [PubMed: 16453726]
49. van der Does C, de Keyzer J, van der Laan M, Driessen AJ. Reconstitution of purified bacterial preprotein translocase in liposomes. Methods Enzymol. 2003; 372:86–98. [PubMed: 14610808]
50. Frank J, et al. SPIDER and WEB: processing and visualization of images in 3D electron microscopy and related fields. J Struct Biol. 1996; 116(1):190–199. [PubMed: 8742743]
51. Phillips JC, et al. Scalable molecular dynamics with NAMD. J Comput Chem. 2005; 26(16):1781–1802. [PubMed: 16222654]
52. Humphrey W, Dalke A, Schulten K. VMD: visual molecular dynamics. J Mol Graph. 1996; 14(1): 33–38. 27–38. [PubMed: 8744570]
53. Pettersen EF, et al. UCSF Chimera—a visualization system for exploratory research and analysis. J Comput Chem. 2004; 25(13):1605–1612. [PubMed: 15264254]

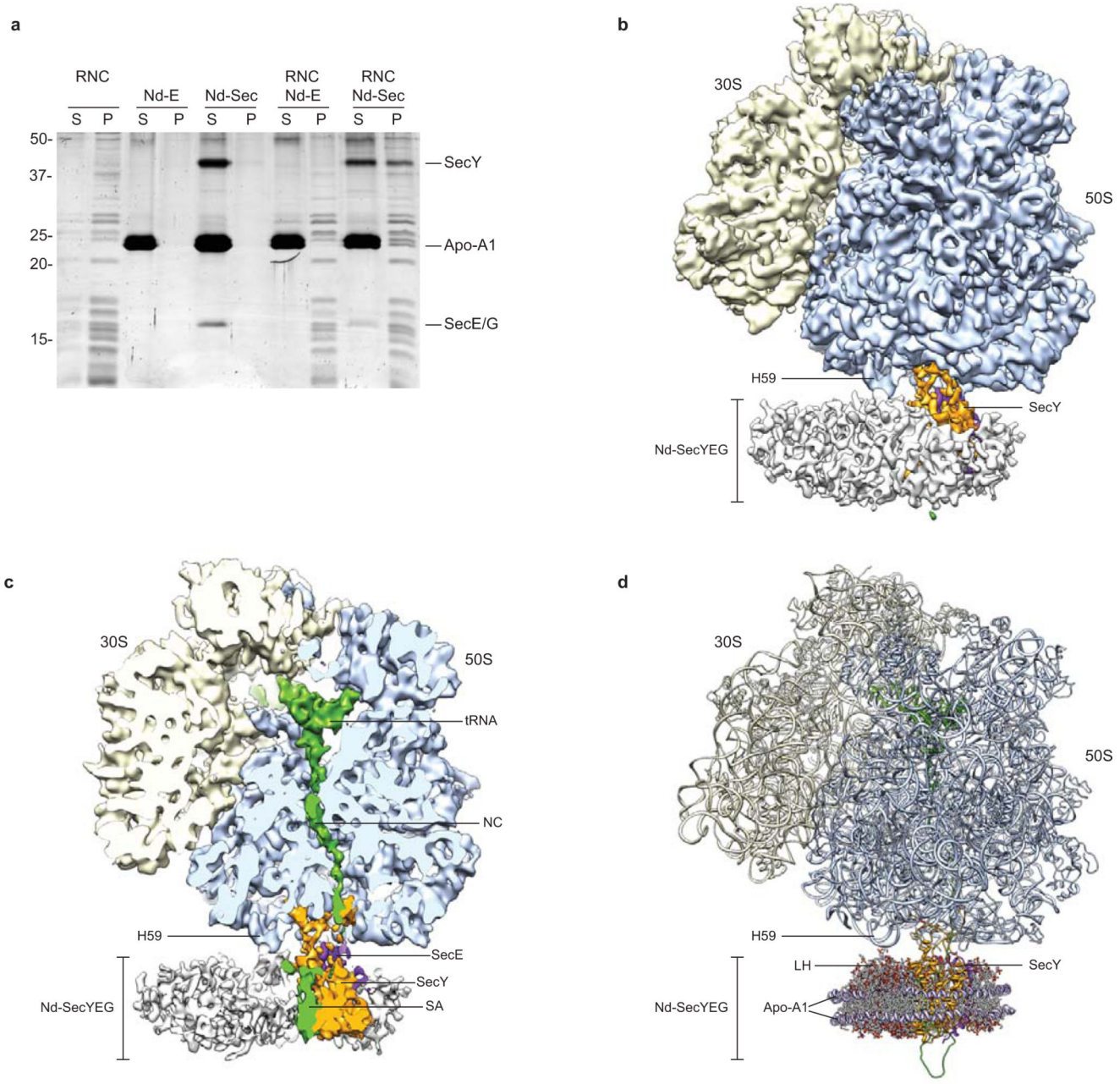

Figure 1. Reconstitution and cryo–EM reconstruction of a 70S RNC–Nd–SecYEG complex

(a) Binding assay using purified RNCs (RNC) with an excess of reconstituted Nd–E and Nd–SecYEG. Supernatant (S) and pellet (P) fractions were analyzed by SDS–polyacrylamide gel electrophoresis and SYPRO orange staining. Nd–SecYEG bind stably to RNCs, whereas Nd–E do not.

(b) Cryo–EM reconstruction of the active 70S–RNC–Nd–SecYEG complex at 7.1 Å resolution. The ribosomal 30S subunit is shown in yellow, the 50S subunit blue, SecY orange, SecE purple, Nanodisc white.

(c) Density as in (b), but cut perpendicularly to the plane of the membrane along the polypeptide exit tunnel, colours as in b with P–site tRNA and nascent polypeptide chain green.

(d) All–atom model of the active 70S–RNC–Nd–SecYEG complex. View and colours as in (b), proteins and RNA in ribbon representation and phospholipids in ball and stick representation with phospholipid headgroups in red/orange and acyl chains white, Apo–A1 in light purple.

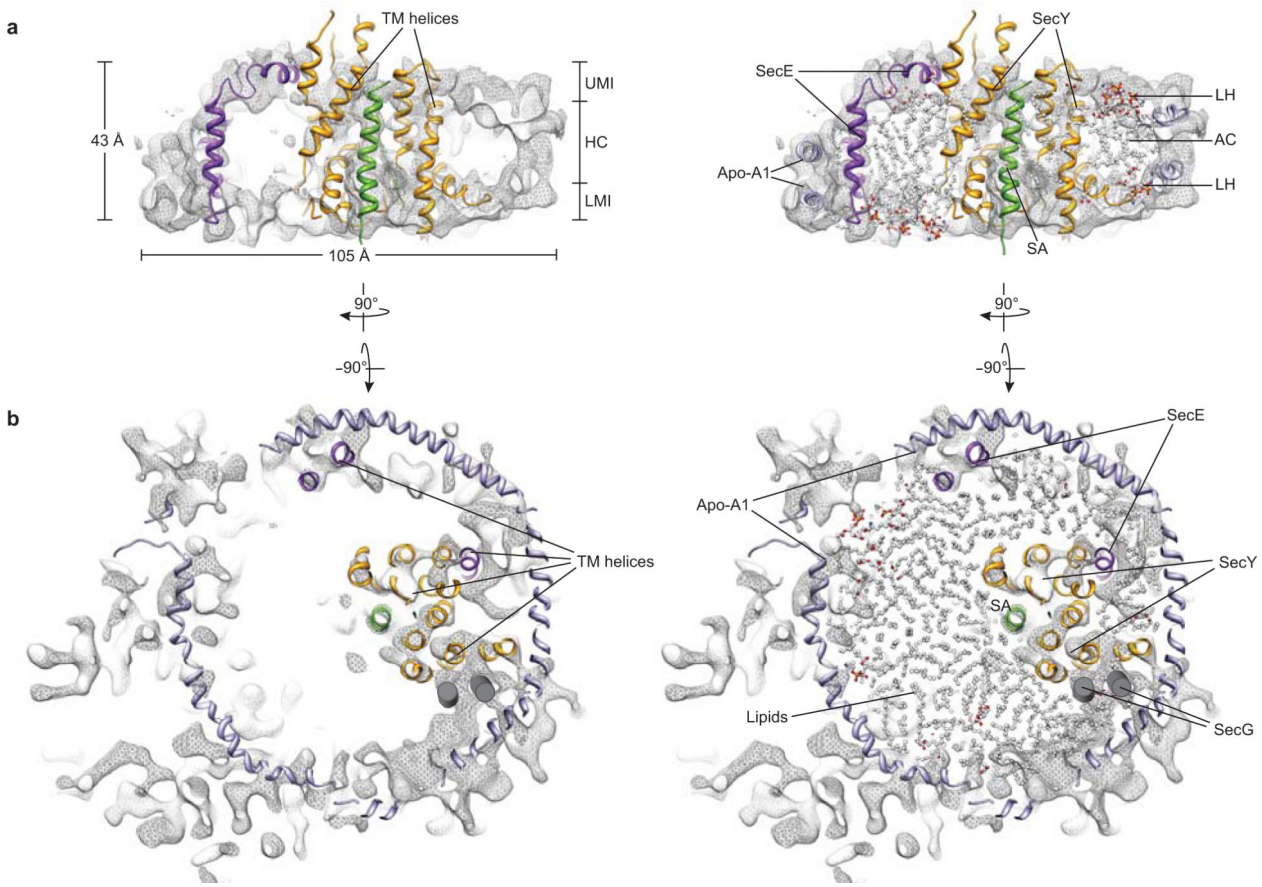

Figure 2. Structure of the Nanodisc

(a) Left: side view cut perpendicular to the plane of the membrane of the isolated electron density of the Nanodisc–SecYEG complex (Nd–SecYEG), showing the lateral gate of SecY. The electron density is represented as a transparent grey mesh with the ribbon representation of the fitted model of a SecY (orange), SecE (purple) and the signal anchor sequence (green). Two layers of density are visible (upper membrane interface, UMI, and lower membrane interface, LMI), separated by a region of lower density (hydrophobic core, HC), containing transmembrane (TM) helices. Dimensions are indicated. Right: Same view, with the fitted Nanodisc–model containing lipids in ball and stick representation. Phospholipid headgroups are red (oxygen) and orange (phosphate), acyl chains white (AC, carbon–hydrogen groups).

(b) Left: horizontal section, sliced within the plane of the membrane within the hydrophobic core of the lipid bilayer. Rod–like features are visible in the interior of the Nanodisc and account for density of a monomeric SecYEG complex. Right: horizontal section with fitted lipids.

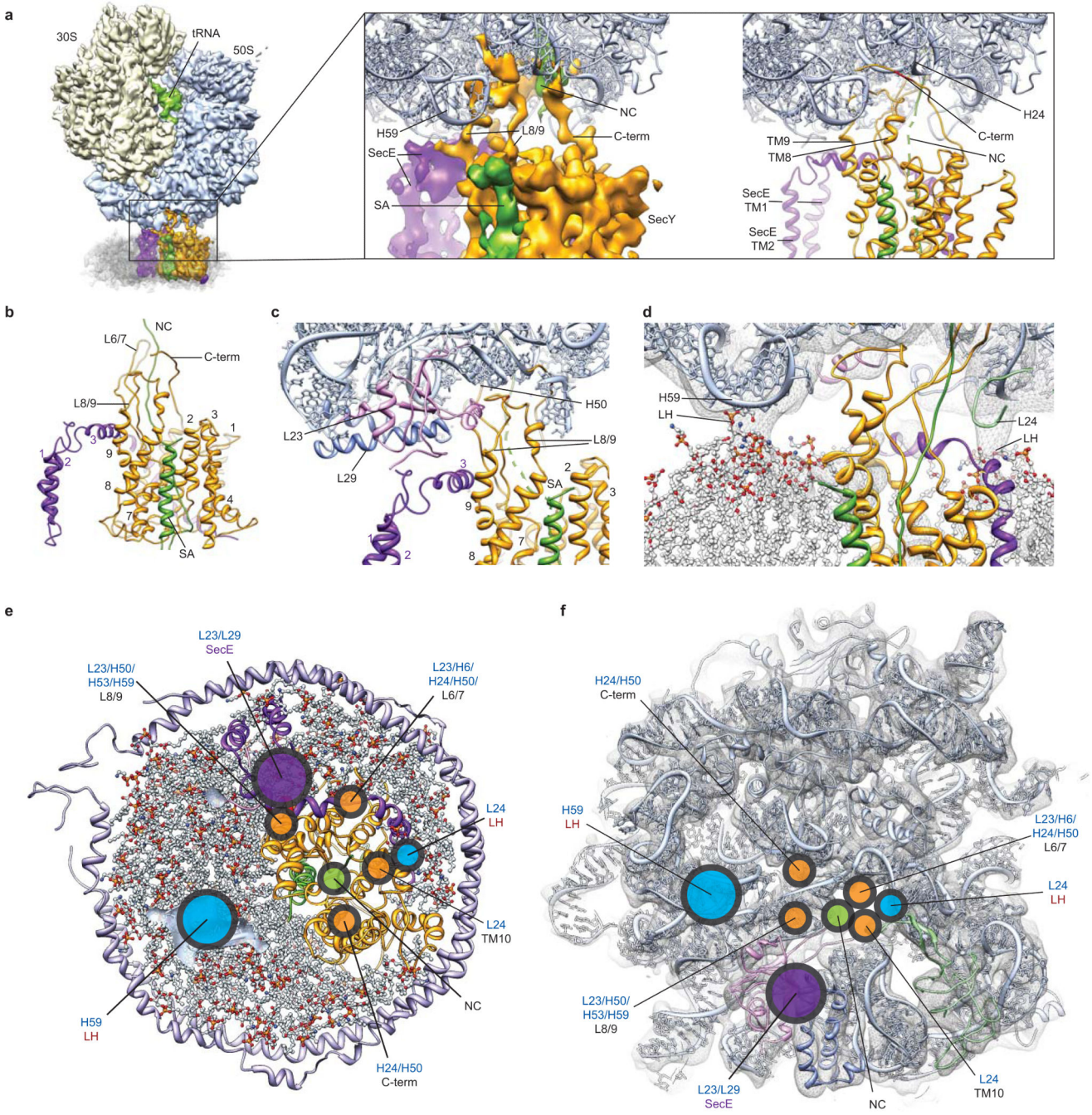

Figure 3. Structure and connections of the membrane–embedded open SecYEG–RNC complex

(a) Cryo–EM reconstruction of the 70S–RNC–Nd–SecYEG complex, colours as in Fig. 1. Insert: molecular model of the 50S subunit with electron density (left) and molecular model for SecYE (right).

(b) Model of the open SecYE complex with a signal anchor (SA, green) residing within the lateral gate, view cut perpendicular to the plane of the membrane.

(c) Close–up of the interaction area of universal ribosomal adaptor site and SecYE.

(d) Molecular model of the ribosome–SecYE–membrane interface with transparent density filtered at 9–10 Å. Lipid headgroups (LH) are indicated.
(e) Cytoplasmic view of the molecular model of the Nd–SecYE complex with contacts to the 50S subunit indicated by circles.
(f) View of the ribosomal tunnel exit site, contact sites as in (e).

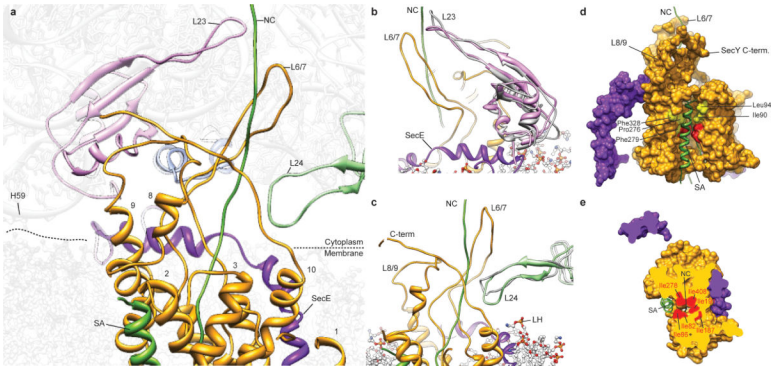

Figure 4. Path of the nascent chain and signal anchor

(a) Section through molecular models of the ribosomal exit tunnel and Nd–SecYE. The nascent chain (NC) with the signal anchor (SA) is shown in green. The dotted line indicates the cytoplasm–membrane interface.

(b) Conformational changes of L23. Comparison of the model of L23 (grey) of an inactive ribosome (PDB: 2i2v) and of L23 (pink) in the presence of a nascent chain (green), SecY (orange), SecE (purple) and lipid headgroups. The intra–tunnel loop of L23 bends towards the nascent chain, close to L6/7 of SecY.

(c) Conformational change of the β–hairpin loop of L24. Comparison of the model of L24 (grey) of an inactive ribosome (PDB: 2i2v) and of L24 (green) in the presence of a nascent chain (green), SecY (orange), SecY C–terminus (SecY C–term), SecE (purple) and lipid headgroups (LH).

(d) View of the lateral gate of SecYE shown as a surface representation. SecY is shown in orange, SecE in purple, the nascent chain in green. Conserved residues of SecY that contribute to the central hydrophobic pore ring are indicated in red and hydrophobic residues of the hydrophobic crevasse that have been found by mutational analysis to be critical for SecY function[5] are indicated in pale yellow.

(e) View of the position of the SA from the cytoplasmic side, sliced within the plane of the membrane. Hydrophobic pore ring residues are indicated in red.

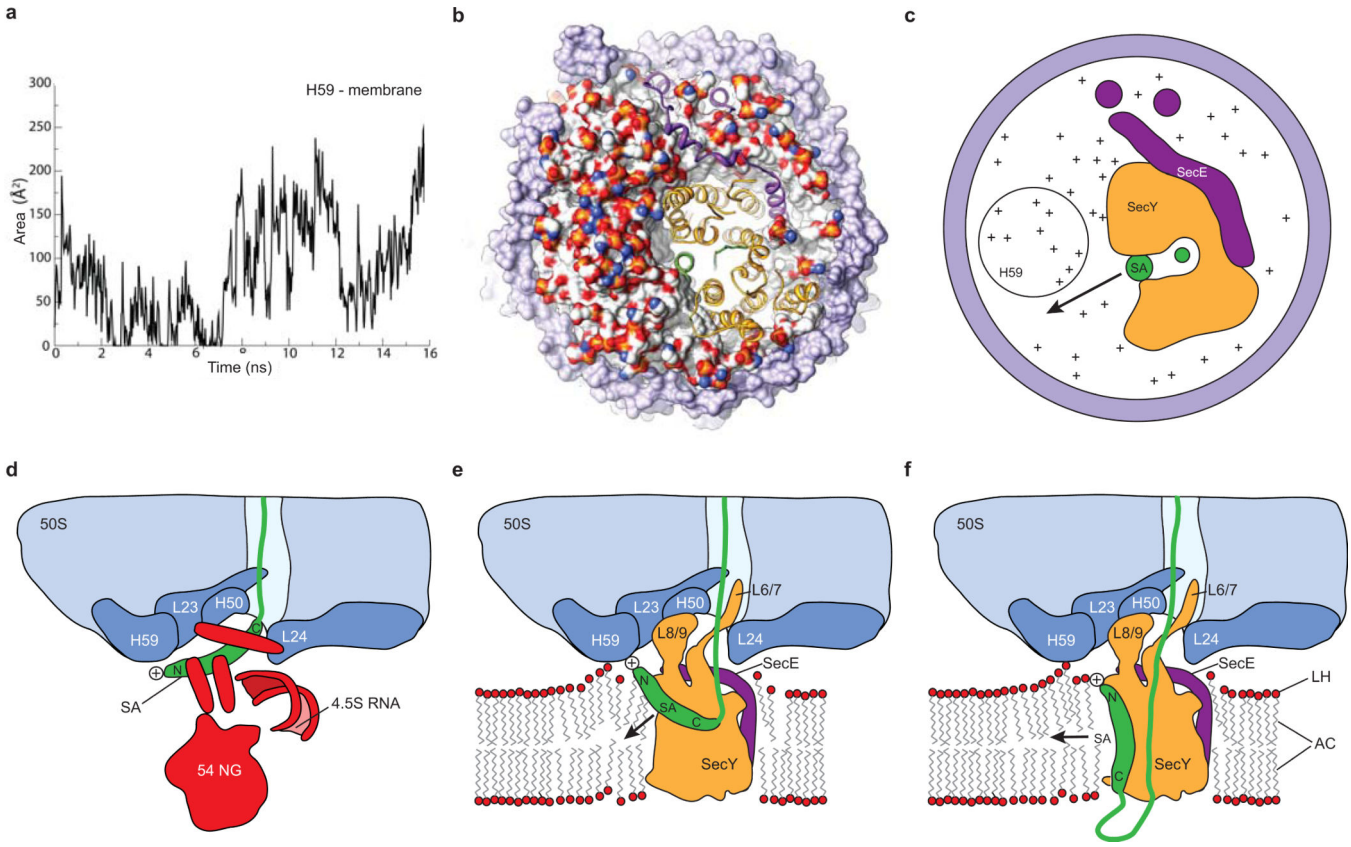

Figure 5. Molecular dynamics simulation and membrane insertion

(a) Plot of surface area formed between lipids and ribosomal helix H59 during the MD simulation.

(b) Surface representation of the Nd–SecYE complex seen from the ribosome after 16 ns MD simulation. Apo–A1 is shown in light purple, SecY in orange, SecE in purple, nascent chain in green and the atoms of the lipid head–groups are coloured in orange (phosphate), red (oxygen) and blue (nitrogen), respectively. Note the accumulation of positive charges in the region close to H59 and the disorder of the lipids forming a groove juxtaposed to the signal anchor.

(c) Schematic depiction of the view in (b) using the same colour code and indicating the probable path of the nascent TM domain for integration into the bilayer.

(d) Schematic depiction of the bacterial 50S ribosomal subunit (blue) bound to SRP (red, 4.5 S RNA and the N–terminal 54–NG domain) in the presence of a signal anchor sequence as observed before[25]. The nascent chain with the signal anchor is shown in green and

(e) Schematic depiction of a hypothetical TM domain insertion intermediate showing the bacterial 50S ribosomal subunit (blue) bound to the SecYEG complex (orange) in the presence of a signal anchor, accessing the hydrophobic lipid phase through a partially open lateral gate.

(f) Schematic depiction of the observed insertion intermediate with the signal anchor TM domain fully inserted into the lateral gate and exposed to the hydrophobic core of the

bilayer. Note the proximity of the SA position as observed in the targeting complex (d) and in the insertion intermediate (e, f).